Geochimica et Cosmochimica Acta, Vol. 69, No. 22, pp. 5317–5331, 2005
Copyright © 2005 Elsevier Ltd
Printed in the USA. All rights reserved
0016-7037/05 $30.00 + .00

doi:10.1016/j.gca.2005.06.026

Stable sulfur isotope partitioning during simulated petroleum formation as determined by hydrous pyrolysis of Ghareb Limestone, Israel

Alon Amrani,[1] Michael D. Lewan,[2] Zeev Aizenshtat[1,*]

[1]Casali Institute of Applied Chemistry and Department of Organic Chemistry, The Hebrew University of Jerusalem, 91904 Jerusalem, Israel
[2]U.S. Geological Survey, Box 25046, MS 977, Denver, CO 80225, USA

(*Received January* 10, 2005; *accepted in revised form June* 27, 2005)

Abstract—Hydrous pyrolysis experiments at 200 to 365°C were carried out on a thermally immature organic-rich limestone containing Type-IIS kerogen from the Ghareb Limestone in North Negev, Israel. This work focuses on the thermal behavior of both organic and inorganic sulfur species and the partitioning of their stable sulfur isotopes among organic and inorganic phases generated during hydrous pyrolyses. Most of the sulfur in the rock (85%) is organic sulfur. The most dominant sulfur transformation is cleavage of organic-bound sulfur to form $H_2S_{(gas)}$. Up to 70% of this organic sulfur is released as $H_2S_{(gas)}$ that is isotopically lighter than the sulfur in the kerogen. Organic sulfur is enriched by up to 2‰ in ^{34}S during thermal maturation compared with the initial $\delta^{34}S$ values. The $\delta^{34}S$ values of the three main organic fractions (kerogen, bitumen and expelled oil) are within 1‰ of one another. No thermochemical sulfate reduction or sulfate formation was observed during the experiments. The early released sulfur reacted with available iron to form secondary pyrite and is the most ^{34}S depleted phase, which is 21‰ lighter than the bulk organic sulfur. The large isotopic fractionation for the early formed H_2S is a result of the system not being in equilibrium. As partial pressure of $H_2S_{(gas)}$ increases, retro reactions with the organic sulfur in the closed system may cause isotope exchange and isotopic homogenization. Part of the $\delta^{34}S$-enriched secondary pyrite decomposes above 300°C resulting in a corresponding decrease in the $\delta^{34}S$ of the remaining pyrite. These results are relevant to interpreting thermal maturation processes and their effect on kerogen-oil-H_2S-pyrite correlations. In particular, the use of pyrite-kerogen $\delta^{34}S$ relations in reconstructing diagenetic conditions of thermally mature rocks is questionable because formation of secondary pyrite during thermal maturation can mask the isotopic signature and quantity of the original diagenetic pyrite. The main transformations of kerogen to bitumen and bitumen to oil can be recorded by using both sulfur content and $\delta^{34}S$ of each phase including the $H_2S_{(gas)}$. H_2S generated in association with oil should be isotopically lighter or similar to oil. It is concluded that small isotopic differentiation obtained between organic and inorganic sulfur species suggests closed-system conditions. Conversely, open-system conditions may cause significant isotopic discrimination between the oil and its source kerogen. The magnitude of this discrimination is suggested to be highly dependent on the availability of iron in a source rock resulting in secondary formation of pyrite. *Copyright © 2005 Elsevier Ltd*

1. INTRODUCTION

The $\delta^{34}S$ of sulfur-rich kerogen and oil is controlled by sulfur incorporation during early diagenesis at relatively low temperatures (Krein, 1993; Anderson and Pratt, 1995; Amrani and Aizenshtat, 2004; Aizenshtat and Amrani, 2004a) and sulfur decomposition and reactions during catagenesis at higher temperatures (Aizenshtat and Amrani, 2004b). At the beginning of the catagenesis stage, Type-IIS kerogen is rich in thermally unstable, organically bound sulfur (8–12 wt%). This low thermal stability is considered a major factor for the early generation of bitumen and heavy oil and the release of large amounts of H_2S (Tannenbaum and Aizenshtat, 1984, 1985; Lewan, 1985; Orr, 1986; Baskin and Peters, 1992; Aizenshtat et al., 1995; Nelson et al., 1995; Koopmans et al., 1998; Lewan, 1998). The effect of these processes on the $\delta^{34}S$ of the organic and inorganic species in the source rock remains to be determined.

Orr (1986) evaluated many oils and their suggested kerogen precursors from the Miocene Monterey Formation. He concluded that the maximum difference between the two was only a 2‰ enrichment of the sulfur into oil relative to that in the source-rock kerogen, suggesting $\delta^{34}S$ is a good parameter for source rock to oil correlations. In contrast, selected oils and kerogens from the Ghareb Limestone and Monterey Formation analyzed by Dinur et al. (1980) and Aizenshtat and Amrani (2004b) showed larger isotopic variations, with the oils being enriched in ^{34}S by as much as 10‰. Only a limited number of experiments monitoring $\delta^{34}S$ changes during thermal maturation of kerogen have been reported. These previous studies (Idiz et al., 1990; Stoler et al., 2003) were conducted under dry pyrolysis conditions in which no expelled oil was produced. Moreover, they did not consider a complete mass balance of sulfur nor the $\delta^{34}S$ of the inorganic sulfur species except for $H_2S_{(gas)}$. Idiz et al. (1990) performed dry pyrolysis experiments in closed ampoules at 300°C on isolated kerogen from the Monterey Formation. These experiments showed small variations of only 2‰ between the sulfur in source kerogen, bitumen and $H_2S_{(gas)}$. Conversely, open-system pyrolysis of a Dead Sea sulfur-rich source rock and isolated kerogens at 300 to 500°C showed larger isotope differences of 10‰ between kerogen, bitumen and hydrogen sulfide (Stoler et al., 2003).

The present study was conducted to follow the $\delta^{34}S$ partitioning of the main organic and inorganic sulfur species during thermal maturation of organic- and sulfur-rich rock of the

* Author to whom correspondence should be addressed (zeev@vms.huji.ac.il).

Table 1. General data describing the experimental temperatures and pressures for 72-h durations, total organic carbon (TOC) and Rock-Eval data (S1, S2, S3 Tmax, and HI) of the unheated and recovered rocks, and the organic products (bitumen, oil and gas) generated in the whole rock pyrolysis experiments.

Reaction temperature °C	Run pressure[b] kPa	TOC Wt. %	S1 mgHC/gRock	S2 mgHC/gRock	S3 $mgCO_2/gC$	Tmax (°C)	HI mgHC/gC	Extracted bitumen mg/gOrig. TOC	Expelled oil mg/gOrig. TOC	Total gas mg/gOrig. TOC
Unheated	—	15.22	1.64	127.21	4.60	402	836	45.9	0.0	0.0
200	1538	15.37	1.36	120.63	3.62	401	785	148.6	0.0	39.4
260	5537	14.52	10.05	114.39	2.82	411	788	588.6	3.3	98.6
300	9605	13.01	21.01	86.51	2.24	423	665	760.3	54.4	180.7
320	12639	11.18	22.98	58.24	2.09	434	521	526.8	150.2	239.8
340	16672	7.89	13.20	22.05	1.69	443	280	190.5	388.9	315.4
365	23671	6.38	7.52	6.11	1.75	449	96	107.3	417.1	436.9
340 dry[a]	3330	11.14	29.98	23.81	1.93	445	214	327.1	0.0	269.4

[a] Experiment with 200g rock and no addition of water.
[b] Absolute pressure, measured within the last 3 hours of the experiment.

Ghareb Limestone, Israel. To better simulate natural thermal maturation, whole rock samples were subjected to hydrous pyrolysis experiments at temperatures ranging between 200 and 365°C for 72 h. Organic-and inorganic-sulfur species were quantified and $\delta^{34}S$ values measured to establish complete mass and isotopic balance of sulfur. These results provide new insights on the behavior of sulfur during thermal maturation and how it partitions into different organic and inorganic phases during petroleum formation.

2. METHODS

2.1. Sample Description

The rock sample used in this study (930616-9) is an organic-rich limestone (15.22 wt% total organic carbon, TOC) containing thermally immature Type-IIS kerogen (atomic S/C = 0.065). The thermal immaturity of the samples is indicated by its low T_{max} of 402°C, high hydrogen index of 836, low production index of 0.01, and low bitumen/TOC ratio of 45.9 mg/g TOC (Table 1). This sample is a massive medium-gray chalky limestone collected from a 17-cm interval, 6 m above the Mishash phosphorite bed in the Nukhel Efe quarry (a.k.a. Rotem deposit, Israel) operated by the Pama Co. (31.076917N and 35.176853E). The sample is blocky with no signs of saprolite rinds or mottled discoloration indicative of pedogenic weathering. The stratigraphy and geology of the Ghareb Limestone are reported in Minster et al. (1992) and Shahar and Wurzburger (1967).

2.2. Hydrous Pyrolysis

The experiments were conducted in stainless-steel Hastalloy C-276 reactors (internal volume: ~1025 cm^3) with carburized surfaces (Lewan, 1993). In each experiment, 200 g of gravel-sized rock chips (0.5–2 cm) were loaded into the reactor with 400 g of distilled water. Calculations based on specific volumes (Lewan, 1993) indicate that this amount of rock would be submerged in liquid water during the entire experiment. After the reactors were sealed, they were filled with 6900 kPa of He and checked for leaks. The pressure was then reduced to 240 kPa of He, and the reactor weighed. Temperatures were monitored with type J thermocouples that were calibrated against national standards at 280, 300, 320, 340, and 360°C. Temperature and pressure variations were manually recorded for 20- to 30-min intervals every 10 to 15 h. Experimental temperatures had standard deviations less than 0.5°C, except for the dry experiment, which had a standard deviation of 0.8°C. All experiments were conducted for 72 h, which was measured from the time the reactors reached the experimental temperature to the time the heaters were turned off. Experimental temperatures were attained between 30 and 60 min. Cooldown time to room temperature took between 18 and 24 h. During cool down, a 50°C decrease occurred within the first 2 h and a 100°C decrease occurred within the first 4.3 h. The dry pyrolysis experiment was conducted as described above but with no added water.

2.3. Kerogen Isolation and Hydrous Pyrolysis

Kerogen was isolated from pulverized rock chips by HCl and HF treatments followed by a heavy liquid separation according to the procedure described by Lewan (1986). The elemental analysis of the isolated kerogen gave 68 wt% C, 8.13 wt% H, 1.9 wt% N, 9.57 wt% O, 12.05 wt% S_{total}, and 11.76 wt% $S_{organic}$. The balance between total sulfur and organic sulfur is pyrite sulfur that was not completely removed by the kerogen isolation procedure. We used 40 g of the kerogen for the hydrous pyrolysis experiments. This amount approximates kerogen content in 200 g of rock that we normally used in our whole rock experiments. Because the isolated kerogen is slightly hydrophobic and difficult to submerge in the reaction water, the weighed amount of kerogen was initially mixed with water using isopropyl alcohol as a wetting agent. The isopropyl alcohol was then removed by sequential rinsing of the wet kerogen in a filter apparatus with distilled water (Lewan, 1997). The final filtered wet kerogen was then added to the reactor with 450 g of distilled water.

2.4. Sampling and Collection of Reaction Products

After the reactor cooled to room temperature, pressure and temperature were recorded. To quantify the sulfide species in the water phase, we decreased the reactor's pressure by releasing the gas into evacuated stainless-steel cylinders with a wide range of volumes to a final absolute pressure of 76–93 kPa (the atmospheric pressure at Denver, Colorado is ~86 kPa). This collection system was allowed to equilibrate for ~1 h before two 51-cm^3 evacuated cylinders were used to take gas samples for compositional analysis and H_2S precipitation. Experiments on the influence of the collection pressure on the sulfur isotopes yield negligible differences with a standard deviation (±0.3‰), almost within the measurement error. The expelled oil generated in the hydrous pyrolysis experiments was collected from the surface of the water at the end of the experiment with a Pasteur pipette and a benzene rinse as described by Lewan (1997). The water recovered from the reactor was filtered (0.45 μm) and an aliquot immediately analyzed for pH and Eh at room temperature. The remaining water was sealed with a minimum amount of air space and was analyzed for sulfide and sulfate within 3 d. Rock chips were removed from the reactor and dried in a vacuum oven at 50°C for 24 h. The dried rock chips were pulverized and bitumen was extracted in a Soxhlet apparatus for 72 h with an azeotropic mixture of CH_2Cl_2 and MeOH. The refluxed solvent was filtered and the bitumen was concentrated by rotary vacuum evaporation and weighed.

The first gas cylinder collected from the reactor was purged with nitrogen into a $AgNO_3$/ NH_4OH solution to precipitate the $H_2S_{(gas)}$ as

Table 2. Sulfur content (mgS/g Total S) of the different sulfur species after 72 hrs hydrous pyrolysis at temperatures noted in table. The maximum error for these results is <10% from the total amount of sulfur in the unheated rock.

Pyrolysis temperature (°C)	Oil (OS)	Bitumen (BS)	Kerogen (KS)	$H_2S_{(gas)}$[c]	$AVS_{(aq)}$	$AVS_{(rock)}$	Total AVS	$SO_{4(aq)}$	$SO_{4(acid\text{-}rock)}$	$SO_{4(w\text{-}rock)}$	Total sulfates	Pyrite (disulfide)
Unheated	—	23.2	851.0	—	—	8.3	8.3	—	23.2	61.3	84.4	33.1
200	0.0	71.2	654.0	104.3	16.6	13.2	29.8	18.2	41.4	18.2	77.8	62.9
260	1.7	220.2	269.9	319.5	39.7	9.9	51.3	16.6	28.1	26.5	71.2	67.9
300	18.2	162.3	89.4	509.9	54.6	11.6	67.9	21.5	29.8	21.5	72.8	81.1
320	41.4	120.9	79.5	538.1	59.6	11.6	71.2	23.2	41.4	8.3	72.8	76.2
340	86.1	48.0	59.6	566.2	61.3	26.5	87.7	28.1	36.4	16.6	81.1	71.2
365	82.8	29.8	41.4	619.2	54.6	33.1	86.1	28.1	21.5	31.5	81.1	59.6
340 (dry)[a]	0.0	74.5	135.8	625.8	—	18.2	18.2	—	46.4	36.4	82.8	61.3
340(iso.Kerogen)[b]	91.1	57.9	66.2	478.5	69.5	5.0	74.5	n.d.[d]	n.d.	n.d.	n.d.	41.4
Unheated iso. kerogen[b]	—	—	761.6	—	—	—	—	—	—	—	—	48

[a] Experiment with 200g rock and no addition of water.
[b] Experiment with 40g isolated kerogen and 450g of distilled water.
[c] The gas quantities were corrected by adjusting the amount of gas to fit the total mass of sulfur in the unheated rock.
[d] Not detected.

Ag_2S. The solution was then filtered and the Ag_2S dried in an oven at 120°C. The second gas cylinder was subjected to gas analysis performed on a Wasson Modiro HP gas chromatograph using a modified version of the ASTM D2650-88 method to determine mole percentages, which were converted to mole and mass units assuming ideal gas behavior at room temperature.

The pulverized and extracted rock from each experiment was sequentially collected and gravimetrically analyzed by the separation procedure of Tuttle et al. (1986). The first step is water extraction of the rock to remove the water soluble sulfate ($SO_4^{2-}{}_{(w\text{-}rock)}$). Then the finely ground 5-g samples were treated in an inert atmosphere with hot 6 N HCl for 30 min to dissolve the acid-soluble sulfates ($SO_{4(acid\text{-}rock)}$) and to form H_2S from the decomposition of monosulfide minerals (acid-volatile sulfur, $AVS_{(rock)}$). The same treatment was applied to the recovered water (20 g) of each experiment to quantitatively collect the dissolved $H_2S_{(aq)}$ and $HS^-{}_{(aq)}$ ($AVS_{(aq)}$) and sulfate ($SO_4^{2-}{}_{(aq)}$). Stannous chloride was added to samples to prevent oxidation of the evolved H_2S by Fe^{3+} which may present in the solution. The H_2S was collected as Ag_2S and the sulfate as $BaSO_4$. Disulfide minerals (mainly pyrite) were reduced in a hot, acidified Cr(II) solution in a nitrogen atmosphere to form H_2S that was collected as Ag_2S. This method has been shown to cause minimal damage to the organic matter in comparison to other methods (Acholla and Orr, 1993). Precision of the sulfur-species analyses was ±10%. The residual matter (mostly kerogen and some silicates) was dried and weighed.

2.5. Speciation of Elemental Sulfur

Elemental sulfur was determined according to Tuttle et al. (1986) by extracting three selected samples (unheated, 200°C, 340°C HP experiments) with acetone. Only trace amounts of elemental sulfur were detected, within the measurement error. All the samples were also Soxhlet extracted with addition of Cu^0 curls as previously described. With the exception of the dry-pyrolysis rock, no formation of CuS occurred, which indicates the absence of elemental sulfur.

2.6. X-Ray Diffraction

Pyrite content was also measured by using X-ray diffraction (XRD) on each residual rock after removing its carbonate minerals with 6 N HCl for 2 h. The residual powdered rock was randomly packed in aluminum holders and analyzed with a Philips diffractometer in Bragg-Brentano geometry using a Cu tube operated at 40 kV and 20 mA with fixed 1-degree divergence slit, graphite-diffracted beam monochromator, scintillation detectors, and NIM-counting electronics. Changes in pyrite content of the samples were determined by comparing the intensity of the 1.633-Å pyrite peak to the intensity of the 26.68-Å quartz peak as a decimal fraction. XRD was also used to detect the presence of pyrrhotite in several of the bitumen-extracted residual rocks. However, a standard of pyrrhotite (research grade Ward's 49V5885) and marbleized Leadville Limestone (Waupaca Northwoods LLC) showed that pyrrhotite concentrations of less than 1 wt% would not be detected by XRD.

2.7. Elemental Analyses and Stable Sulfur Isotope Measurements

The expelled oil, extracted bitumen and kerogen (residual matter after sulfur specification) were subjected to elemental analysis for C, H, N, and S using a Carlo Erba 1106 elemental analyzer. Analytical error was ±0.15 wt% for carbon and ±0.3 wt% for sulfur. $\delta^{34}S$ of the precipitated Ag_2S, and $BaSO_4$, and the organic samples were measured by a continuous-flow elemental analyzer connected to a Finnigan /Mat Delta Plus stable-isotope ratio monitoring mass spectrometer (EA-irmMS). Sulfur isotope compositions are expressed as per mil (‰) deviations from V-CDT (Vienna Canyon Diablo Troilite) standard using the conventional delta notation with a standard deviation better than 0.3‰ ($n \geq 2$). The measurements were directly calibrated against sulfur isotopic standards IAEA-S-1 (Ag_2S, −0.3‰) and NBS-127 ($BaSO_4$, +20.3‰) with a standard deviation less than 0.2‰ ($n \geq 3$).

2.8. Mass Balance

Mass balance calculations were carried out based on the quantitative results for all analyzed sulfur species. The total mass of sulfur in each experiment was corrected to the unheated total sulfur value by adjusting the amount of S in H_2S of the gas phase, because the gas measurements have the largest expected error that in some cases exceeded 10%. H_2S dissolved in the oil could be part of this balance problem. However, a positive correlation was not observed between H_2S mass error and amount of oil generated. In all cases, the total sulfur mass balance error was less than 10%. The isotopic mass balance for total $\delta^{34}S$ resulting from the calculations of all experiments had a standard deviation of 0.4‰.

3. RESULTS

3.1. Character of Initial Sulfur in Unheated Rock

Elemental sulfur could not be detected in the unheated rock. This is in agreement with other studies of this area (Dinur et al., 1980). A relatively low pyrite S content of ~3 wt% of total S in the rock was measured (Table 2). The pyrite in this unheated sample is ca.30‰ isotopically lighter than the organic sulfur (Table 3). This difference is in the upper range for $\Delta_{\text{organic-pyrite}}$ for immature samples of this

Table 3. Sulfur $\delta^{34}S$ (‰) data values measure for each sulfur species after 72 hrs hydrous pyrolysis at temperatures noted in table. Measurement error is better than ±0.3‰ (n>2).

Pyrolysis temperature (°C)	Oil (OS)	Bitumen (BS)	Kerogen (KS)	H_2S(gas)	$AVS_{(aq)}$	$AVS_{(rock)}$	Total AVS	$SO_{4(aq)}$	$SO_{4(acid\text{-}rock)}$	$SO_{4(w\text{-}rock)}$	Total sulfates	Pyrite (disulfide)
unheated	—	2.6	0.6			−4.6	−4.6		6.7	−5.7	−2.3	−29.9
200	—	0.8	0.7	−0.5	−1.3	0.0	−0.7	−5.7	1.3	−5.5	−1.9	−25.2
260	0.7	0.8	1.0	1.1	1.3	−3.1	0.4	−6.1	2.9	−5.6	−2.2	−23.6
300	1.6	1.5	1.6	0.2	0.5	0.4	0.5	−5.9	3.6	−5.3	−1.8	−21.6
320	1.7	1.4	2.0	0.9	1.0	−0.5	0.7	−5.9	1.5	−5.1	−1.6	−22.7
340	2.4	1.9	2.6	1.2	0.2	0.2	0.2	−5.7	2.5	−5.4	−1.9	−23.6
365	2.3	2.0	2.1	2.0	1.4	−2.2	0.1	−5.5	5.5	−5.4	−2.5	−27.8
340 dry[a]	—	2.3	2.0	0.5		−0.5	−0.5	—	0.9	−5.7	−2.0	−25.4
340(iso.Kerogen)[b]	1.9	1.2	n.a.[c]	1.7	1.6	0.6	1.5	—	—	—	—	−29.3
Unheated iso.kerogen[b]		—	0.6	—	—	—	—	—	—	—	—	−29.2

[a] Experiment with 200g rock and no addition of water.
[b] Experiment with 40g isolated kerogen and 450g of distilled water.
[c] measurment not available.

area (Dinur et al., 1980; Aizenshtat and Amrani, 2004a) as well as other locations of immature sedimentary rocks (Anderson and Pratt, 1995). The very large sulfur isotopic difference might indicate a very early open system for sulfate reducing bacteria (SRB), which later became a closed system resulting in much heavier $\delta^{34}S$ values of sulfate (Aizenshtat and Amrani, 2004a). This explanation is supported by the $\delta^{34}S$ results of sulfates in the present study. Sulfate S is only ~8% of total S with $\delta^{34}S$ values ranging between −5.7 to + 6.7 (Table 3). These relatively low $\delta^{34}S$ values could not have resulted from residual marine sulfate (+20 ± 2‰). The extensive sulfate reduction evident in the formation of Type-IIS kerogen should have left the residual sulfate even heavier than the original marine values. The big $\delta^{34}S$ difference between the water-soluble (-5.7‰) and acid-soluble sulfates (+6.7‰) in the unheated rock can be rationalized by different times of crystallization. The acid-soluble sulfate is mostly associated with carbonates, which trapped sulfate during the earlier stages of formation (Staudt and Schoonen, 1995) whereas the water-soluble sulfate could be from secondary oxidation of organic sulfur or sulfide minerals. This is supported by the similar $\delta^{34}S$ values of water-soluble sulfate and the mineral sulfides ($AVS_{(rock)}$, Table 3). Only a small amount of acid-volatile sulfide ($AVS_{(rock)}$) minerals could be detected (< 0.1% w/w of total S). We suggest that the pyrite is formed early, whereas the $AVS_{(rock)}$ is formed later with secondary organic sulfur enrichment. This is contrary to the results reported for the Monterey Formation (California, USA; Miocene) by Zaback and Pratt (1992). It is possible that the timing of SRB activity and the closing of the water-sediment interface were different in the case of the Senonian basins, hence the much heavier range of pyrite $\delta^{34}S$ values. The bitumen fraction of the unheated rock contains 2.4% of the total sulfur in the sample with a $\delta^{34}S$ value that is heavier than the kerogen by 2‰ (Table 3). In most of the samples from this area (Mishor Rotem), the bitumen was ^{34}S-enriched relative to the kerogen. However, the $\delta^{34}S$ values recorded for the various sulfur species of different sites in the Dead Sea area show wide variability (Aizenshtat and Amrani, 2004a)

3.2. Organic Sulfur

Hydrous pyrolysis experiments generate five phases that contain organic sulfur: kerogen (KS), bitumen (BS), expelled oil (OS), water-soluble organic compounds, and sulfur containing gas compounds. We assume that the latter two are quantitatively negligible, and therefore, they are not addressed in the present study. Table 1 shows the variations in these organic phases with increasing experimental temperatures. The amount of bitumen increases with temperature to 300°C and then decreases as generated expelled oil continues to increase with increasing temperatures. This bitumen-oil relationship has been previously observed in hydrous pyrolysis experiments and explained by kerogen initially decomposing to a polar-enriched bitumen and subsequent decomposition of bitumen to hydrocarbon-enriched oil (Lewan, 1985). With the exception of bitumen above 300°C, the atomic S/C ratio decreases in all the organic phases with increasing experimental temperature (Fig. 1a). The residual kerogen in the lower-temperature experiments has the highest S/C and from 340°C the bitumen has the higher S/C values. The wt% S in each organic phase (Fig. 1b) shows a similar decrease with increasing temperature for the oil and kerogen but the sulfur content of the oil remains the same or higher than the kerogen. Similar results have been reported for hydrous pyrolysis experiments on Monterey kerogens (Baskin and Peters, 1992; Nelson et al., 1995). The bitumen above 300°C shows an increase in sulfur with increasing temperature and this increase explains the essentially constant atomic S/C ratios observed at the higher temperatures (Fig. 1a). Table 2 shows that more sulfur is retained in the organic matter of the dry pyrolysis experiment than in the hydrous pyrolysis experiment at 340°C. This observation has been previously reported and attributed to sulfur cross-linking reactions being promoted under dry pyrolysis conditions (Lewan, 1997).

Figure 1c shows the effect of experimental temperature on the $\delta^{34}S$ of the organic species. It is clear from the results and in accordance with organic maturity parameters (Table 1) that as thermal maturity increases, the organic sulfur phases are enriched in ^{34}S. Except for the unheated sample, the bitumen is always lighter than the residual kerogen, and the expelled oil becomes heavier than the kerogen above 340°C. In general, the

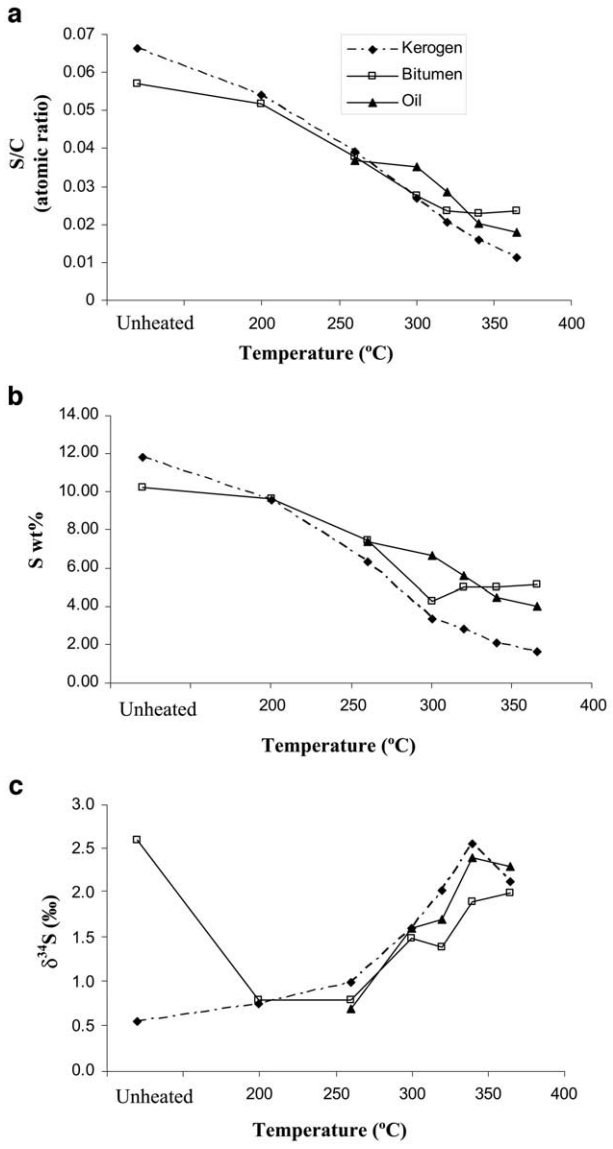

Fig. 1. Organic sulfur in residual kerogen, bitumen, and oil as a function of hydrous pyrolysis temperature. (a) Atomic S/C atomic ratios. (b) S wt%. (c) $\delta^{34}S$ (‰).

$\delta^{34}S$ differences between the various organic species are very small (less than 1‰).

The overall change between the $\delta^{34}S$ of oil and the organic sulfur in the kerogen of the unheated sample is about + 2‰. This small value was also observed in dry pyrolysis experiments of sulfur-rich kerogens from the Monterey Formation (Idiz et al., 1990).

3.3. Sulfides

As shown in Table 2, the amount of sulfides in the gas phase ($H_2S_{(gas)}$) is about one order of magnitude higher than the other two sulfide phases ($AVS_{(aq)}$ and $AVS_{(rock)}$). $H_2S_{(gas)}$ has the highest mass of all the other sulfur species above 300°C. There is a steep increase in the amount of $H_2S_{(gas)}$ from 200 to 300°C and a gentler increase at the higher temperatures (Fig. 2a). The $\delta^{34}S$ of the $H_2S_{(gas)}$ shows a broken trend of ^{34}S enrichment with increasing temperature (Fig. 2b). ^{34}S enrichment occurs from 200 to 260°C and abruptly decreases at 300°C before continuing to increase at the higher temperatures. This overall ^{34}S enrichment is consistent with the $\delta^{34}S$ trend of the organic sulfur, but the $H_2S_{(gas)}$ is generally lighter than the organic sulfur species. $AVS_{(aq)}$ increases with increasing temperature to 340°C and decreases at 365°C (Fig. 3a). $\delta^{34}S$ of the $AVS_{(aq)}$ increases steeply between 200 and 260°C and then unsystematically fluctuates between 0.2 and 1.4 ‰ at the higher temperatures (Fig. 3b). Relatively small amounts of $AVS_{(rock)}$ exist in the unheated rock (Table 2) and no significant change occurs until 340°C. At this temperature, the amount of $AVS_{(rock)}$ begins increasing (Fig. 3a), which suggests formation of metal sulfides like FeS. Pyrrhotite or other FeS-crystalline forms was not detected in the recovered rocks using XRD analyses. However, pyrrhotite is not detectable in concentrations equal to or less than 1 wt%. According to the amount of $AVS_{(rock)}$ in our samples, the maximum amount of pyrrhotite that could form is less than 0.3 wt%. Therefore, the XRD results do not exclude the presence of pyrrhotite. The initial $\delta^{34}S$ of $AVS_{(rock)}$ is −4.6‰. This value is lighter than the initial organic sulfur (+0.6‰) and much heavier than the pyritic sulfur (-29.9‰). There are big fluctuations in the $\delta^{34}S$ values of $AVS_{(rock)}$ as a function of the experiment temperatures with no apparent trend (Fig. 3b). Mass balance calculations were made (Eqn. 1) for total AVS forms (i.e., $AVS_{(rock)}$ + $AVS_{(aq)}$). The amounts of this summation ($AVS_{(total)}$) increase with increasing temperature. The $\delta^{34}S$ of the $AVS_{(total)}$ increases steeply to 320°C and then remains relatively constant at higher temperatures (Fig. 3b).

In the dry pyrolysis experiment, $\delta^{34}S$ of $H_2S_{(gas)}$ and $AVS_{(rock)}$ are lighter than in the hydrous experiment (Table 3). With more of the sulfur being retained in the rock under dry conditions (Table 2) as a result of more cross-linking, it is expected that the $\delta^{34}S$ of $H_2S_{(gas)}$ and $AVS_{(rock)}$ would be heavier under hydrous conditions. $\delta^{34}S$ of $H_2S_{(gas)}$ and $AVS_{(rock)}$ of the isolated-kerogen hydrous experiment are respectively heavier by only 0.3 and 0.4 ‰ than those of the whole-rock hydrous experiment at 340°C (Table 3). This difference is within the measurement error.

3.4. Sulfates

Figure 4a shows the quantitative distribution of sulfate species vs. experimental temperature. Except for the unheated and 365°C samples, the $SO_4^{2-}{}_{(w\text{-}rock)}$ and $SO_4^{2-}{}_{(acid\text{-}rock)}$ are essentially mirror images with no systematic trends at the intermediate temperatures. The amount of $SO_4^{2-}{}_{(aq)}$ remains essentially constant from 200 to 260°C, but increases steadily at the higher temperatures. The total amount of sulfates shows a gentle decrease from the unheated sample to 260°C, a constant concentration from 260 to 320°C, an increase to 340°C, and a constant concentration to 365°C. The unheated $\delta^{34}S$ values of the different sulfate species vary significantly from −5.7‰ for $SO_4^{2-}{}_{(w\text{-}rock)}$ to + 6.7‰ for $SO_4^{2-}{}_{(acid\text{-}rock)}$ (Table 3). As shown in Figure 4b, the water-soluble forms of sulfate have similar $\delta^{34}S$ values that suggest they have a similar source. There is essentially no change in their $\delta^{34}S$ with increasing temperature. In contrast, acid-soluble sulfate $\delta^{34}S$ values are

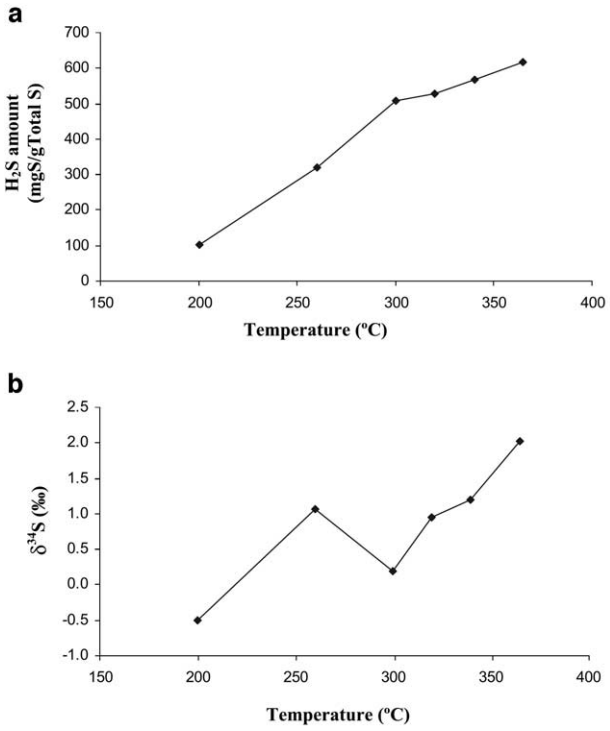

Fig. 2. H_2S in the gas phase ($H_2S_{(gas)}$) as a function of hydrous pyrolysis temperature (°C). (a) Amount of $H_2S_{(gas)}$ in mgS/g Total S, where Total S refers to total sulfur in the original unheated rock. (b) $\delta^{34}S$ (‰) values of $H_2S_{(gas)}$.

consistently heavier and change dramatically with temperature. Although this change is not systematic with temperature there is a good negative correlation between the $\delta^{34}S$ and amount of $SO_4^{2-}{}_{(acid\text{-}rock)}$ (Fig. 4c). This suggests addition of ^{34}S-depleted sulfur species into $SO_4^{2-}{}_{(acid\text{-}rock)}$ crystalline form. No isotopic exchange with other sulfur species is suggested because the total sulfate mass-balance calculation shows small fluctuations within a standard deviation of ± 0.3‰. The only transformations were between the sulfate species with addition or depletion of isotopically lighter water-soluble sulfates and no recrystallization of the initial acid-soluble sulfate. Therefore, we conclude that no significant thermochemical sulfate reduction (TSR) occurred within the source rock under our experimental conditions. The dry pyrolysis experiment has similar results to the hydrous experiment at the same temperature (i.e., 340°C) with no change in the amount and isotopic values of total sulfates.

3.5. Pyrite

Disulfide minerals are referred to as pyrite in this paper because XRD analyses detected no other disulfide minerals. As expected (Anderson and Pratt, 1995; Aizenshtat and Amrani, 2004a), pyrite is the most ^{34}S-depleted species relative to all other sulfur species. The $\delta^{34}S$ of pyrite in the unheated rock is −29.9‰ (Table 3). With increasing experimental temperature (Fig. 5a), pyrite becomes isotopically heavier to a maximum of −21.6‰ at 300°C followed by decreasing ^{34}S values at the higher temperatures. However, it does not return to the initial $\delta^{34}S$ value of the pyrite in the unheated rock. Because pyrite is the most ^{34}S-depleted species in the system, this change in $\delta^{34}S$ may be the result of (i) isotope exchange with heavier sulfur species or (ii) addition of heavier species of sulfur cleaved off the organic matter during the hydrous pyrolysis experiments to form secondary pyrite. The first explanation (i) is ruled out because the nonpyritic sulfur species should be ^{34}S depleted according to mass balance calculations, however, these sulfur species become ^{34}S enriched (Table 3). The second explanation (ii) is more likely and is supported by the increase and decrease in the amount of pyrite that parallels the changes in $\delta^{34}S$ of the pyrite (Fig. 5a and 5b). The pyrite quantity positively correlates with the $\delta^{34}S$ values (Fig. 5c). This suggests secondary pyrite formation from sulfur species that are isotopically heavier than the initial pyrite at the lower temperatures and then, as the temperature rises above 300°C, pyrite starts to decompose. This is supported by the ratio of pyrite to indigenous quartz determined by XRD analysis in the recovered rocks (Fig. 5d). The results show a similar trend to that in Figure 5 with the exception of peak secondary pyrite formation occurring at 320°C and not at 300°C, as shown by the quantitative and isotopic analyses. This discrepancy is considered to be a result of the semi-quantitative character of the XRD method. The dry pyrolysis experiment showed slightly lower pyrite formation and $\delta^{34}S$

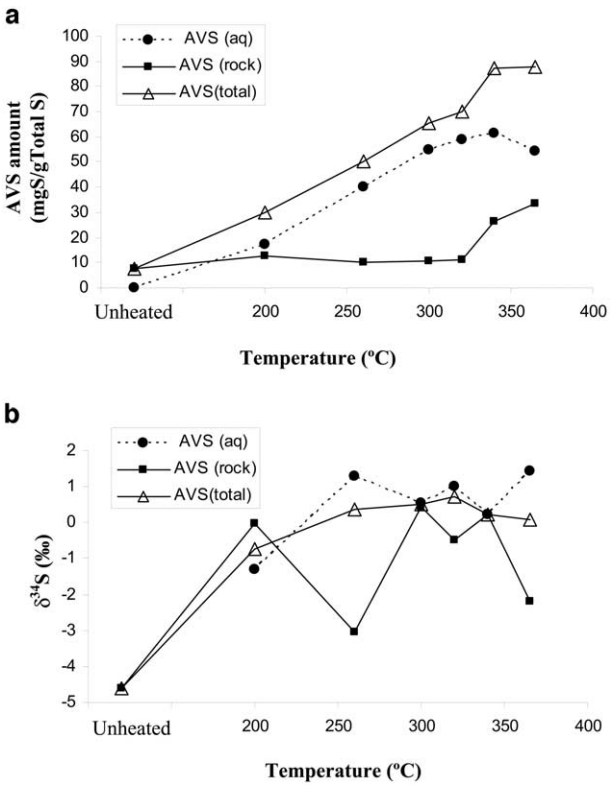

Fig. 3. Acid-volatile sulfur species in the recovered water ($AVS_{(aq)}$), acid-volatile monosulfides in the recovered rock, ($AVS_{(rock)}$), and summation of acid-volatile sulfur in the water and the rock ($AVS_{(total)}$) as a function of hydrous pyrolysis temperature (°C). (a) Amount in mg S/g Total S in original rock. (b) $\delta^{34}S$ (‰) values.

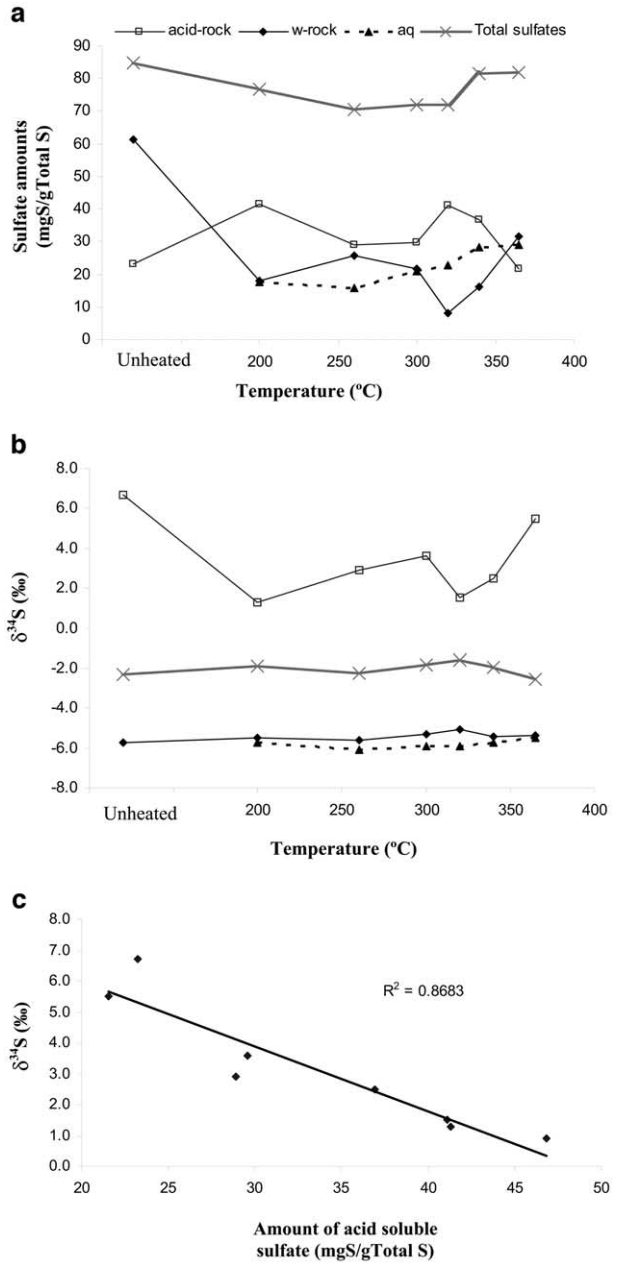

Fig. 4. Sulfate in the recovered water ($SO_{4(aq)}$), water-soluble sulfate from the rock ($SO_{4(w\text{-}rock)}$) and acid-soluble sulfate in the rock ($SO_{4(acid\text{-}rock)}$) and total sulfate as a function of hydrous pyrolysis temperature (°C). (a) Amounts in mg S/g Total S in original rock. (b) $\delta^{34}S$ (‰) values. (c) $\delta^{34}S$ (‰) of acid-soluble sulfate as a function of its amount in mg S/g Total S in original rock.

in comparison with the hydrous experiment at the same temperature.

3.6. Sulfur Mass Balance

The isotope mass balance was calculated according to the general equation

$$\delta_T = x\delta_{SO_4} + y\delta_{pyrite} + z\delta_{organic} \ldots \quad (1)$$

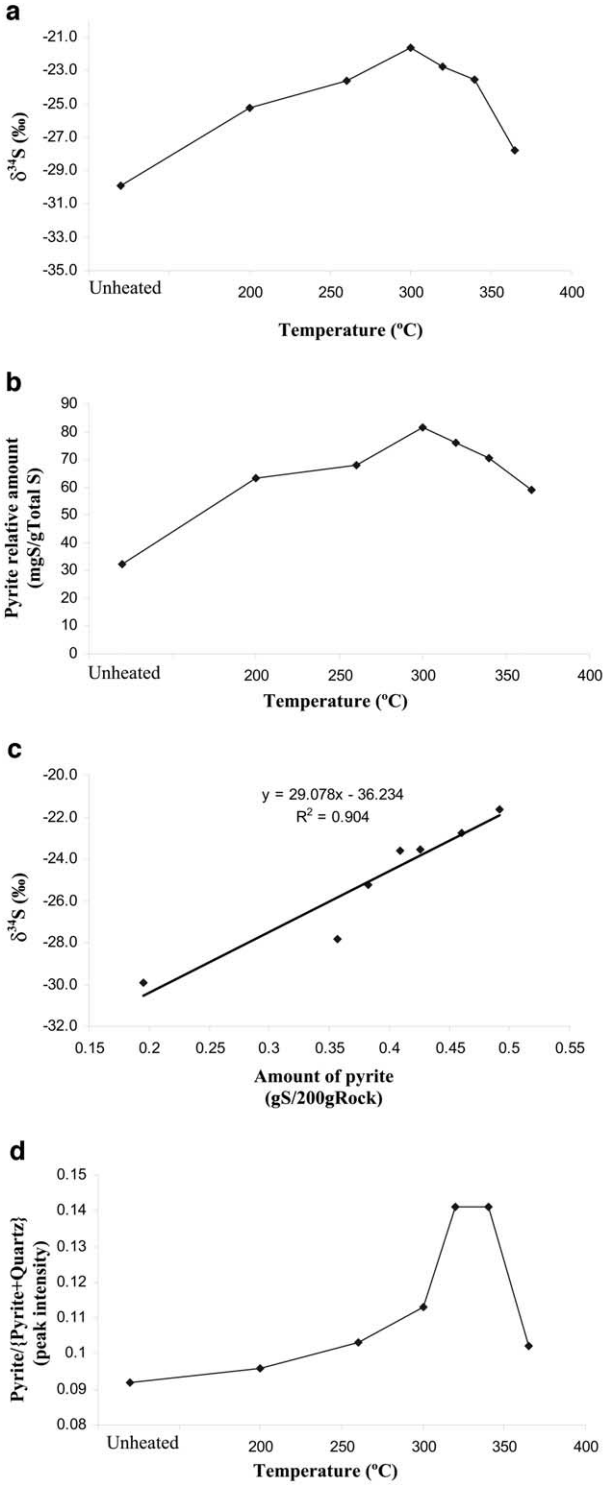

Fig. 5. Disulfite (pyrite) as a function of hydrous pyrolysis temperature (°C). (a) $\delta^{34}S$ (‰) values. (b) Amounts in mg S/g Total S in original rock. (c) $\delta^{34}S$ (‰) of pyrite as a function of amount of pyrite (g S/200 g rock). (d) Semiquantification of pyrite relative to indigenous quartz by X-ray diffraction.

where δ values are in ‰ for each sulfur species, x,y,z. . ., which represent the mass fractions of sulfur in each form. The calculated results showed very similar $\delta^{34}S$ values for all experi-

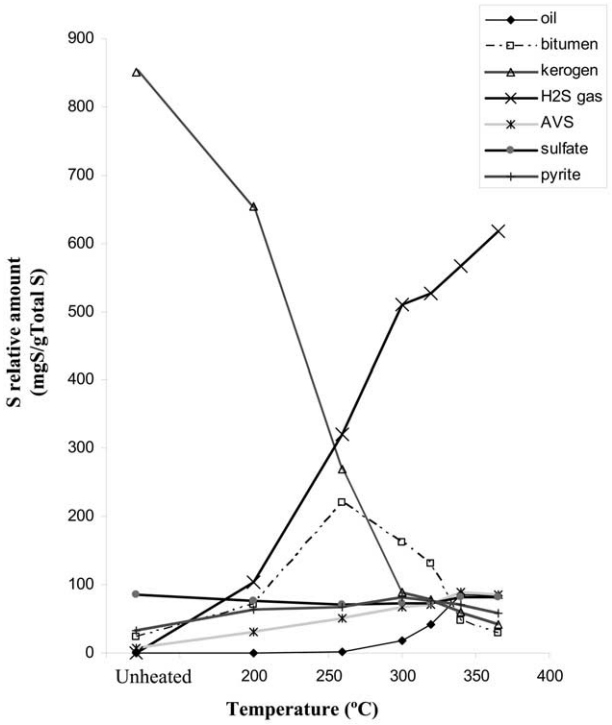

Fig. 6. Sulfur content in each sulfur species in mg S/g Total S in original rock as a function of hydrous pyrolysis temperature (°C) and the unheated sample.

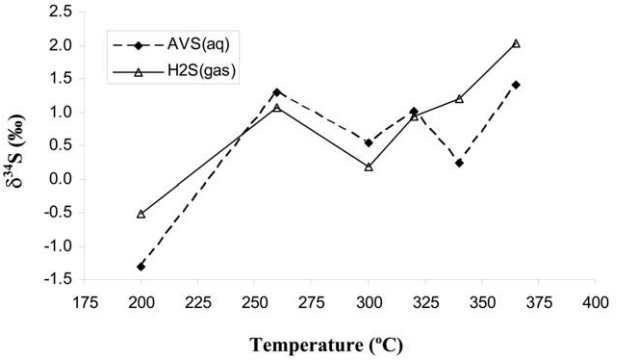

Fig. 7. $\delta^{34}S$ (‰) values of $H_2S_{(gas)}$ and AVS(aq) as a function of hydrous pyrolysis temperature (°C).

ments with an average of −0.9 ± 0.4‰. This compares well with the unheated whole rock $\delta^{34}S$ value of −0.7 ± 0.2‰.

The distribution of all sulfur species during the hydrous pyrolysis experiments is characterized mainly by the sharp decrease of sulfur content in the kerogen and the formation of large quantities of H_2S_{gas} during this process (Fig. 6).

The major loss of sulfur is from the kerogen, which contains ~85 to 4 wt % of total sulfur in the rock. Most of this lost sulfur occurs as H_2S_{gas} that accounts for as much as ~62 wt % of the total sulfur and 70 wt% of the organic sulfur (365°C). This massive loss of sulfur is responsible for the $\delta^{34}S$ changes in all sulfur species (except sulfate) during thermal alteration. The rest of the sulfur is divided between the organic bonded sulfur, pyrite, sulfate and AVS (Fig. 6). The AVS fraction increases with increasing experimental temperature up to 9 wt %. Sulfate S is ~8 wt % of total S with very small fluctuations as the experiment temperatures increase. The pyritic sulfur fraction starts at 3.3 wt % and peaks at 300°C reaching 8.3 wt % of total rock sulfur. The bitumen sulfur increases up to 22 wt % at 260°C, and then decreases to 3 wt % at the highest pyrolysis temperature (365°C). The expelled oil is formed mostly from decomposition of the bitumen. The expelled oil sulfur reaches the highest value at 340°C (8.6 wt %) and decreases slightly to 8.3 wt % at 365°C.

4. DISCUSSION

4.1. Isotopic Equilibrium: Open or Closed System

The present set of hydrous pyrolysis experiments was conducted in a closed thermally controlled system. Hence, reactive sulfur species may equilibrate under in situ conditions (Seewald, 2001). These reactions in turn can lead to isotopic homogenization of the different sulfur species in the system. During our experiments, high amounts (Table 2) of sulfides are produced and maintained through several reversible processes that include different sulfur species and phases. The most obvious equilibrium reactions in our system are between $H_2S_{(gas)}$ and $AVS_{(aq)}$ as follows:

$$H_2S_{(gas)} \rightleftarrows H_2S_{(aq)} \quad (2)$$

$$H_2S_{(aq)} \rightleftarrows HS^-_{(aq)} + H^+_{(aq)} \quad (3)$$

In each of our experiments, we produce three very different pressure and temperature conditions. One is during hydrous pyrolysis, where both experimental temperature and pressure are maintained for 72 h. The second is during cooling of the reactor (at least 18 h) resulting in decreasing temperature and pressure. The third is after cool down when pressure decreases while collecting the generated gases (76–93 kPa; see Experimental). In each stage, there are different equilibrium constants and therefore, different partitioning between the gas and aqueous phases. Because we did not perform in situ measurements we deal with the overall changes resulting from these three stages. Comparison of the $\delta^{34}S$ of $AVS_{(aq)}$ species to the $H_2S_{(gas)}$ (Fig. 7) shows similar values (except for the 340°C experiment), which suggests an isotopic equilibrium between these sulfide species has been reached. In contrast, the metal sulfides represented by the $AVS_{(rock)}$ show no correlation between their $\delta^{34}S$ values and those of the other sulfides (Table 3). This lack of correlation suggests that the $AVS_{(rock)}$ within the bitumen-impregnated rock may not be in equilibrium with the other sulfides at the collection conditions. Laboratory experiments with ^{35}S-labeled sulfur species showed rapid (less than 1 h) isotope exchange between H_2S, S, S_x^{-2} and FeS at a pH 7.6 and 20°C (Fossing and Jorgensen, 1990). They suggest that this isotope exchange occurs via polysulfide formation. When no elemental sulfur is present in the system no polysulfides are formed (under reducing conditions). Hence, HS^- and FeS reach only partial isotope exchange, at a relatively slow rate (24 h). In our experiments, only negligible amounts of elemental sulfur were detected. Moreover, at pH values of 6.6 ± 0.1 that prevail in our experimental system at ambient conditions during product collection, polysulfides are not stable

(Schwarzenbach and Fisher, 1960; Boulegue, 1978; Boulegue and Michard, 1978). This can explain the $\delta^{34}S$ differences between metal sulfides and other sulfide species in our system.

Significant amounts of $H_2S_{(gas)}$ that we collected under reduced pressure are actually dissolved in the water phase and organic phases at the experimental temperatures. At these experimental temperatures, two main processes occur simultaneously: (1) Sulfur cleavage from the organic matter as radicals extract hydrogen to form stable bisulfide or hydrogen sulfide; and (2) Sulfur introduction into organic matter mainly via radical attack (Aizenshtat et al., 1995; Krein and Aizenshtat, 1995). The rate of the first process must be higher than the latter because there is a decrease in the sulfur content of the organic matter with increasing temperature (Fig. 1a,b). These processes yield stabilized organic sulfur mainly as thiophene functionality (Nelson et al., 1995). Seewald (2001) suggested aqueous organic compounds and iron-sulfide minerals (pyrite, pyrrohotite, magnetite) attained metastable thermodynamic equilibrium under hydrous pyrolysis conditions (300 to 350°C). During the stabilization and rereaction of sulfur with the organic matter (Krein and Aizenshtat, 1995), isotopic exchange with the large sulfur pool involving HS^-, H_2S, and FeS could occur under equilibration conditions. In a closed system, this would minimize the larger possible isotope kinetic effect during the cleavage of C-S and S-S bonds (Aizenshtat and Amrani, 2004b; Amrani et al., 2005b).

In contrast, in an open-system the generated sulfur would be immediately removed from the system and a maximum isotope fractionation would occur. Previous experiments conducted under open-system conditions using rocks and isolated kerogen with high-sulfur contents, showed a much higher isotopic discrimination between the released H_2S and the residual organic sulfur fractions of kerogen and bitumen (Stoler et al., 2003). Similar results were obtained for a synthetic polysulfide cross-linked polymer in open-system pyrolysis (Amrani et al., 2005b). The gradual increase in temperature (1 to 10°C/m.y.), the limited void space in fine-grained rocks (5 to 10% porosity), and high lithostatic pressures (70 to 150 MPa) in the subsurface make it difficult to categorically assign a closed or open system to natural thermal maturation and petroleum generation. Noting the amount of isotopic fractionation in natural subsurface sulfur species may help determine the level of openness in natural geological systems.

4.2. Pyrite Stability

4.2.1. Secondary Pyrite Formation and Decomposition

It has been shown that the secondary pyrite formed at temperatures of 300°C or less is ^{34}S enriched compared with the unheated pyrite (Fig. 5a). Formation of the secondary pyrite requires a source of additional iron in the rock. This is supported by the observation that no secondary pyrite appears to have formed in the isolated-kerogen experiment at 340°C. The amount of pyrite in this experiment is ~40 wt% less than that in the whole-rock experiment at the same temperature (Table 2). In addition, the $\delta^{34}S$ of the pyrite in the isolated-kerogen experiment (-29.3‰) is similar to that of the original unheated kerogen (-29.2‰).

Figures 5a and 5b show that pyrite decomposition above 300°C leads to ^{34}S-depletion. This trend can be interpreted to result from the isotopically heavier secondary pyrite being preferentially decomposed relative to the original pyrite. It is possible that this secondary pyrite is less stable or more susceptible to decomposition. Previous studies on pyrite structure and its abundance in samples of bituminous rocks of the Dead Sea area have reported that pyrite occurs as both framboids and single crystals ($<50\mu$), which are typically coated with organic matter (Spiro, 1980; Spiro et al., 1983a,b). This coating may protect the original pyrite from decomposition at the higher temperatures. Conversely, some of the secondary pyrite may reside in the contact zone of the water-rock interface making it more susceptible to aqueous dissolution resulting in its preferential degradation.

Seewald et al. (1994) suggested pyrite recrystallizes to pyrrhotite between 325 and 400°C in hydrous pyrolysis experiments according to the following equation:

$$FeS_2 + H_2 \rightarrow FeS + H_2S \quad (4)$$

The presence of molecular hydrogen and negative Eh values (Eh = −345 to −373 mV) measured at room temperature during product collection suggest that reducing conditions existed and therefore, could have been favorable for pyrrhotite formation. Figure 8 shows the sharp increase in $AVS_{(rock)}$ as the pyrite abundance decreases at temperatures higher than 300°C. Calculation of pyrite S mass loss from the peak formation at 300 to 365°C and the S mass added to the $AVS_{(rock)}$, reveal similar quantities (~0.15 g). $AVS_{(rock)}$ represents sulfide containing minerals, which includes pyrrhotite. If pyrrhotite is the main mineral being formed, then an additional source of Fe is needed. According to Eqn. 5, 1 mol of pyrite produces 2 mol of iron monosulfide:

$$FeS_2 + Fe^{2+} + H_2 \rightarrow 2FeS + 2H^+ \quad (5)$$

Similar to the needed Fe for formation of the secondary pyrite, the Fe needed to form an iron monosulfide like pyrrhotite is likely to have come from the rock. Unlike other carbonaceous rocks of the Zefe Efe' deposit, the Ghareb Limestone is relatively rich in Fe with values from 0.8 to 1.1 wt% (Spiro, 1980). The peak formation of the secondary pyrite requires only a quarter of this Fe, with the remaining Fe being more than sufficient to source formation of pyrrhotite.

4.2.2. Geochemical Implications for Secondary Pyrite Formation

Pyrite is believed to be the isotopic marker for bacterial reduction of sulfate during diagenesis (Anderson and Pratt, 1995; Goldhaber, 2004; Aizenshtat and Amrani, 2004a). However, the results of the present study provide new insights on the applicability of pyrite as an isotopic marker in thermally mature rocks. In natural maturation, thermal decomposition of pyrite is not expected, because the catagenic temperatures are much lower than in our experiments. However, other chemical conditions may develop and effect pyrite stability (Seewald, 2001). It is suggested that during catagenetic processes, secondary and isotopically heavier pyrite is formed (< 300°C) as long as available iron is present, and therefore, the isotopic difference between pyrite and organic sulfur decreases. This

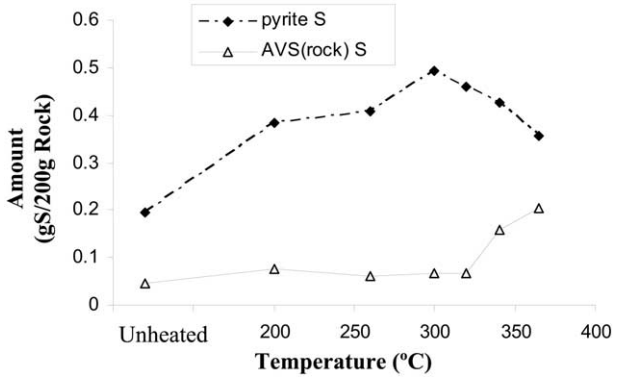

Fig. 8. Amounts of pyrite and acid-volatile monosulfides in the rock ($AVS_{(rock)}$) (g S/200 g rock) as a function of hydrous pyrolysis temperature (°C).

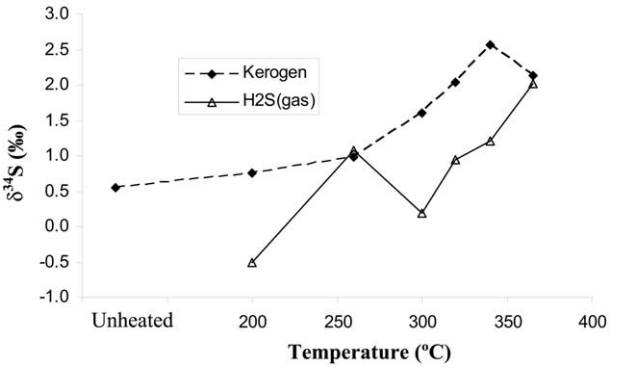

Fig. 9. $\delta^{34}S$ (‰) values of residual kerogen sulfur (KS) and $H_2S_{(gas)}$ as a function of hydrous pyrolysis temperature (°C).

may erase the original diagenetic isotopic signature and quantity of pyrite and cause erroneous interpretations of the early diagenetic conditions of a rock.

4.3. $\delta^{34}S$ Value of Thermally Formed Early Cleaved Sulfur

4.3.1. Direct Measurement

The kinetic-isotope effect (e.g., Coplen, 1993) suggests weaker bonds will preferentially break, i.e., ^{32}S-S, C-^{32}S, with the cleaved sulfur being depleted in ^{34}S and the residual organic sulfur being enriched in ^{34}S. To evaluate this kinetic-isotope effect during thermal maturation, we have to evaluate the $\delta^{34}S$ of the early unequilibrated sulfur species that were cleaved from the thermally matured organic matter. Figure 9 shows that $H_2S_{(gas)}$ produced at the end of each heating experiment is always lighter than the kerogen by up to 1.4‰ with the exception of the 260°C experiment. At the lowest experimental temperature (200°C), the $\delta^{34}S$ of the released $H_2S_{(gas)}$ was −0.5‰, which is 1.1‰ lighter than the original kerogen that produced it. Isotope mass balance of $AVS_{(total)}$ shows $\delta^{34}S$ values up to 2‰ lighter than the initial organic sulfur. Since the present experimental system is closed, the early released and lighter isotopes may equilibrate with other sulfur species (as discussed previously) leading to a smaller apparent fractionation.

In the 340°C experiment, a new silver coated gasket was used to seal the reactor. Upon opening the reactor at the end of the experiment, Ag_2S crystals were observed on the reactor gasket. The $\delta^{34}S$ of these crystals was −2.2‰, which is more depleted in ^{34}S than the $H_2S_{(gas)}$ by 3.4‰, the unheated kerogen by 2.8‰, and the heated residual kerogen by 4.8‰. The amount of the sulfur deposited on the silver-coated gasket is small and cannot balance the isotopic fractionation of the other sulfur species (e.g., H_2S and organic). However, assuming it represents early formed $H_2S_{(gas)}$, it provides evidence that the early released sulfur is isotopically lighter than the later-formed sulfur in the system. The magnitude of this early fractionation for synthetic polysulfide cross-linked polymers and isolated kerogen has been shown to be in the range of 6 to13.9‰ as determined by pyrolysis experiments under closed and open vessel conditions (130 to 300°C) for short time periods (Amrani et al., 2005a; b).

4.3.2. Isotope Mass Balance Calculations of Secondary Pyrite $\delta^{34}S$

It is evident from the experimental results that virtually all sulfur species (except sulfate) become isotopically heavier relative to the unheated rock with increasing thermal maturation (Table 3). However, a good isotope mass balance is obtained for all the experiments and indicates that lighter isotopes must be incorporated into one or more of the different sulfur phases. As discussed in the pyrite section, secondary pyrite formation has been observed. The sulfur source for this pyrite is probably sulfur species that are cleaved from the kerogen. To determine the isotopic value of this additional sulfur, isotopic mass-balance calculations were made on pyrite. These calculations are based on the assumption that the original pyrite did not react and therefore has the initial unheated pyrite $\delta^{34}S$ value. The following isotope mass balance equation was used:

$$\delta^{34}S_{\text{secondary pyrite}} = \left(\delta^{34}S_{\text{pyrite (T+i)}} - \left(1-x\right)\delta^{34}S_{\text{pyrite (T)}}\right)/\left(x\right) \quad (6)$$

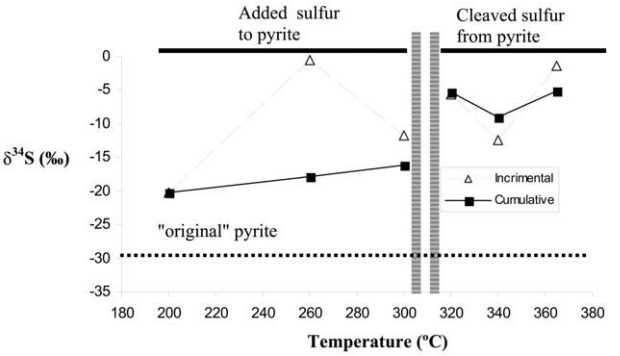

Fig. 10. $\delta^{34}S$ (‰) values of the incremental and cumulative sulfur added to form secondary pyrite as a function of hydrous pyrolysis temperature to and including 300°C. Above 300°C, the incremental and cumulative $\delta^{34}S$ (‰) values represent the released sulfur formed by secondary pyrite decomposition. These values were calculated according to mass balance Eqns. 6 and 7 based on data presented Tables 2 and 3.

Where T = previous temperature, i = increment temperature, and x = the secondary pyrite S mass fraction added to the pyrite at the previous pyrolysis temperature. The $\delta^{34}S$ values of the additional sulfur according to these calculations are shown in Figure 10. The early production of secondary pyrite at 200°C gave a calculated $\delta^{34}S$ value of −20.3‰ and the largest quantity of added sulfur. The incremental secondary pyrite between 200 and 260°C has a much heavier $\delta^{34}S$ of −0.6‰ that decreases at higher temperatures (260 to 300°C) to −12.4‰. The cumulative secondary pyrite formed from unheated to 300°C has a calculated $\delta^{34}S$ of −16.1‰. These calculations suggest that the early cleavage S from the kerogen is isotopically much lighter than what was measured in any of the other phases. These values can balance the other isotopically heavier sulfur species in the organic and gas phases.

The decomposition of pyrite above 300°C releases isotopically heavier sulfur in comparison to the unheated pyrite as determined by the following mass balance equation:

$$\delta^{34}S_{\text{released pyrite}} = \left(\delta^{34}S_{\text{pyrite (T)}} - \left(1 - y\right)\delta^{34}S_{\text{pyrite (T+i)}}\right)/y \quad (7)$$

where y is the pyrite S mass fraction, released from the pyrite at a previous temperature greater than 300°C. According to these calculations, the released sulfur value is between −1.4‰ to −12.4‰ (Fig. 10), which suggests secondary pyrite preferentially decomposes at higher temperatures.

The results of these mass-balance calculations demonstrate the important role of sulfide minerals in trapping the early released and light sulfur isotopes that were produced by thermal decompositions of organic sulfur. The removal of light sulfur isotopes from the system gradually increases the ^{34}S enrichment of the residual sulfur fractions, and especially the organic sulfur. The magnitude of this fractionation is dependent on the amount of available iron or other metals in the system.

4.4. Reaction Mechanisms of Organic Phases

The present work identifies trends that are based on the transformation of kerogen to bitumen and bitumen to oil (Lewan, 1983; Baskin and Peters, 1992) as well as the coinciding sulfur-functionality transformations. The initial steep part of $H_2S_{(gas)}$ generation below 300°C (Fig. 2a) mainly represents the cleavage of weak poly sulfide (S-S) bonds in the kerogen as it decomposes to bitumen (Nelson et al., 1995). Initially, the poly ^{32}S-^{32}S bonds will be preferentially broken to give ^{34}S-depleted $H_2S_{(gas)}$ at relatively low temperatures (Fig. 2b). This early-cleaved sulfur reacts with available iron to produce secondary pyrite (Fig. 5b) with the excess being released to the water and gas phases. As the reaction proceeds with increasing temperature, more of the ^{32}S-^{34}S bonds will be broken and the $H_2S_{(gas)}$ will become more ^{34}S enriched. During this stage, some of the kerogen sulfur is also transferred to the bitumen, probably as C-S bonds in the polar fraction are cleaved. As shown in Table 1, the amount of bitumen is still increasing at 300°C, but some of it is breaking down to a hydrocarbon-enriched oil. This represents the breaking of more C-S bonds in the bitumen, which results in free radicals that initiate the low-thermal stress cleavage of C-C bonds in bitumen to form oil (Lewan, 1998). This C-C cleavage may also be enhanced by sulfide minerals (Seewald, 2001) that formed and decomposed (Fig. 8). The cleavage of C-S bonds in bitumen to oil would generate less H_2S than the cleavage of S-S bonds from kerogen to bitumen (200 to 300°C) as shown in Figure 2a by the gentler slope. The $\delta^{34}S$ plot in Figure 2b suggests this new source of H_2S is initially very ^{34}S depleted, which when added to the early poly S-S source results in a lowering of the $\delta^{34}S$ value. As more C-S bonds are broken in the bitumen with increasing thermal maturation, more of the stable C-^{34}S bonds break, which results in an increase in the $\delta^{34}S$ value as shown in Figure 2b. As shown in Figure 6, the sulfur content in the bitumen first increases to 260°C and the $\delta^{34}S$ of the generated bitumen remains constant (Fig. 1b). As thermal maturity increases, the sulfur in the bitumen decreases as the bitumen decomposes to oil. During this process, the bitumen $\delta^{34}S$ becomes lighter compared to the oil due to the more stable C-^{34}S bonds that are broken. The amount of S in the oil that is forming from the decomposition of the bitumen increases as shown in Figure 6 to 340°C and remains essentially constant to 365°C. The $\delta^{34}S$ values of the oil during this stage become heavier, and are heavier than coexisting bitumen with increasing thermal maturation. When the oil sulfur yield becomes essentially constant from 340 to 365°C, so do the $\delta^{34}S$ values. The similar quantities of H_2S generated in the dry pyrolysis (gas = 6.26 wt% S) and in the hydrous experiment (aqueous + gas = 6.28 wt% S) indicate that the added water in hydrous pyrolysis experiments is not a critical source of hydrogen for the formation of H_2S (Table 2).

4.5. Implications for Petroleum Correlations

4.5.1. Hydrogen Sulfide–Oil Correlation

It is evident from our experiments that the thermally formed $H_2S_{(gas)}$ is ^{34}S depleted in comparison to the coexisting oil, although the difference is relatively small. Therefore, we would expect that if the sole source of $H_2S_{(gas)}$ is the thermal desulfurization of organic matter in a source rock, $\delta^{34}S$ of the generated $H_2S_{(gas)}$ will be the same or slightly depleted in ^{34}S compared to generated oils under closed-system conditions. There are only a few studies that report $\delta^{34}S$ of oil and associated hydrogen sulfide in natural reservoirs. These studies involved well-developed oil fields (10–30 yr), which could affect the original isotopic characteristic of the gases (Vredenburgh and Cheney, 1971). Therefore, caution should be used in interpreting these data. In most of these $\delta^{34}S$ measurements, $H_2S_{(gas)}$ was found to have values close to those of its coexisting oil (Thode et al., 1958) or ^{34}S enriched (Vredenburgh and Cheney, 1971; Orr, 1974). Thode et al. (1958) explain this by small isotopic fractionation between oil and hydrogen sulfide. Vredenburgh and Cheney (1971) explained the ^{34}S enrichment of hydrogen sulfide by preferential removal of the ^{32}S fraction of the $H_2S_{(gas)}$ by differential migration of the oil and gas or by chemical reaction with metals in the carrier or reservoir beds during migration. However, it is known that only negligible fractionation of the sulfur occurs in the formation of metal sulfides (up to 1‰, e.g., Price and Shieh, 1979; Wilkin and Barnes, 1996; Bottcher et al., 1998) and therefore, even if portions of the gas reacted with metals, $\delta^{34}S$ of the residual gas would not change significantly. Moreover, additional thermally

cleaved H_2S will be ^{34}S depleted in comparison the organic sulfur as discussed previously.

Additional problems in using $\delta^{34}S$ in correlating $H_2S_{(gas)}$ to oil may arise from reservoir processes that introduce microbial sources of H_2S or TSR. Microbial production of H_2S requires lower temperatures and in most cases generates a distinctly light $\delta^{34}S$ value. In deep high-temperature reservoirs, TSR is the most reasonable way to produce H_2S that is isotopically heavier than the coexisting oils (Orr, 1974; Worden et al., 2003). As a result of these potential additional sources of H_2S in reservoirs, $\delta^{34}S$ correlations of hydrogen sulfide to oil are not likely to be reliable.

4.5.2. Source Rock–Oil Correlation

Two main hypotheses on the $\delta^{34}S$ relationship between source rock and oil can be considered. The first is that only negligible $\delta^{34}S$ fractionation occurs during thermal cleavage of organic sulfur, and therefore, all sulfur fractions (except for pyrite and sulfate) in a given maturation system have similar $\delta^{34}S$ values (Orr, 1974, 1986). Orr (1986) concluded that generated oils have up to 2‰ enrichment relative to their source-rock kerogen. This suggests that $\delta^{34}S$ is a good parameter for source rock-to-oil correlations. Laboratory pyrolyses further supported this assumption (Idiz et al., 1990). Similarly, the results of the present study show fractionation within 1‰ between kerogen, bitumen and expelled-oil. Despite the agreement of these results with this hypothesis, some cautionary points need to be made. The present study shows that $\delta^{34}S$ fractionation during early thermal cleavage of organic sulfur is large, with values as high as 21‰. Therefore, under some natural conditions, greater differences in $\delta^{34}S$ values between genetically related oils and H_2S gas might be possible, particularly in the early stages of oil and gas generation. It is also important to realize that the $\delta^{34}S$ of oil is typically the collective product of different lateral and stratigraphic facies of a maturing source rock. Therefore, the certainty of an oil correlation will always be dependent on how representative the analyzed rock samples are of the maturing source rock and its organic facies. This caution is a concern in all oil-to-source rock correlations (Waples and Curiale, 1999) and not restricted to the use of $\delta^{34}S$ values.

The other hypothesis is that there is a large negative fractionation between H_2S and organic-sulfur fractions, and as a result, the organic sulfur fractions become ^{34}S enriched (Aizenshtat and Amrani, 2004b). This hypothesis is based on the results of open-system pyrolyses on isolated kerogen and bituminous rocks of the Dead Sea area (Stoler et al., 2003) and on closed- and open-system pyrolysis experiments on a synthetic polymer and an isolated kerogen (Amrani et al., 2005a). Results from these experiments show large isotopic discrimination between $H_2S_{(gas)}$ and the residual organic sulfur. Additional support can be given by the finding that oils found in the Dead Sea area are generally significantly ^{34}S enriched in comparison to their source kerogens (e.g., Aizenshtat and Amrani, 2004b). A more open system is suggested to be responsible for this greater fractionation.

During thermal maturation of Type-IIS kerogen, high amounts of $H_2S_{(gas)}$ are produced. We report in the present study that more than 70 wt% of the original organic sulfur of the kerogen (Fig. 6) is converted to $H_2S_{(gas)}$, which is dissolved into the water, expelled oil and bitumen at elevated temperatures (>300°C). These results suggest that in natural systems the huge amounts of generated H_2S have to accumulate somewhere or escape from the system. Accumulation could occur through formation of metal sulfides (Worden et al., 2003) similar to the secondary formation of pyrite in our experiments. This process can happen in the source rock or during migration in carrier beds that contain available iron or other metals (Seewald, 2003). In addition, H_2S is highly soluble in water (Suleimenov and Krupp, 1994) and much of it could be lost as an aqueous phase to formation waters of carrier beds or to adjoining formation waters by diffusion. Preferential loss of isotopically light H_2S during maturation and migration from its source kerogen could yield ^{34}S-enriched oil. In most cases, petroleum reservoirs are spatially separated from their source rock indicates that the generation, expulsion, and migration of oil are open-system processes (Seewald, 2003). This may cause significant isotopic discrimination between the oil and its source kerogen. The magnitude of this discrimination is suggested to be highly dependent on the mineral facies of each reservoir and carrier bed. Therefore, correlation between oil and its source rock using $\delta^{34}S$ measurements can serve as a reliable tool only when thermal maturation and petroleum generation are in a more closed system.

4.5.3. Oil-Oil Correlation

$\delta^{34}S$ values of the early- and late-generated expelled oils have a narrow range (0.7 to 2.4 ‰), which is in general agreement with some studies of natural crude oils. Thode and Monster (1970) reported $\delta^{34}S$ values with a standard deviation of ±2.6‰ for oils from 12 fields extending over a distance of 320 km in northern Iraq. Gaffney et al. (1980) also reported $\delta^{34}S$ values with a small standard deviation of ±2.1‰ for Jurassic oils of different thermal maturities from an unspecified basin. Oils in the Winnipeg–Red River, Bakken-Madison, and Pennsylvanian-Tyler systems in the Williston basin had $\delta^{34}S$ standard deviations of ±1.2, ±2.8, and ±0.7 ‰, respectively (Thode, 1981). Vredenburgh and Cheney (1971) reported a $\delta^{34}S$ standard deviation of ±2.8 ‰ for Pennsylvanian-Permian crude oils representing a wide range of thermal maturities in the Wind River Basin. Manowitz et al. (1990) reported a $\delta^{34}S$ standard deviation of ±1.8 ‰ for Bolivar coastal field oils that extend over 2500 km^2 in northern Venezuela. Oils and heavy oils from the Dead Sea area that are considered to be sourced from the Ghareb Limestone have a mean $\delta^{34}S$ value of 1.6 ‰ with a standard deviation of ±1.2 ‰ (Aizenshtat and Amrani, 2004b). These natural oil values compare well with the 0.7 to 2.4 ‰ $\delta^{34}S$ values for the oils generated from the sample of Ghareb Limestone used in this study (Table 3).

Although this agreement between laboratory-generated oils and natural crude oils encourages the use of $\delta^{34}S$ in oil-oil correlations, some caution should be taken in correlations that involve oils that have been altered by water washing and biodegradation. Asphaltic tars in the Dead Sea area show a much wider range of $\delta^{34}S$ values (0.0 ± 4.7‰, Aizenshtat and Amrani, 2004b) than observed in the laboratory-generated oils and natural crude oils. This wider range of values may be a result of variations in the $\delta^{34}S$ of kerogen locally responsible

for the asphaltic tars or alteration of the original oils or bitumen by water washing and biodegradation. Thode (1981) shows alteration of Williston-basin oils by this type of process results in $\delta^{34}S$ values becoming heavier by almost 7‰. Another consideration in using $\delta^{34}S$ values for oil-oil correlations is thermal maturity of the oil. Although changes in $\delta^{34}S$ values of the hydrous-pyrolysis oils became heavier by only 1.7‰, greater fractionations due to thermal maturation of natural crude oils have been reported. Orr (1974) reports mean $\delta^{34}S$ values changing from −3.5 to 6.3 ‰ in oils from the Big Horn Basin with increasing thermal maturity. Vredenburgh and Cheney (1971) reports mean $\delta^{34}S$ values from −5.0 to + 5.0, from high-sulfur, low API gravity shallow crude oils to the low sulfur higher gravity oils below present depths of 3300 m, respectively. As discussed earlier, this larger difference in some natural crude oils may be related to a more open-system during natural oil generation than the closed-system used in hydrous pyrolysis. Lastly, $\delta^{34}S$ variations in different organic facies of a maturing source rock may also be responsible for the larger variations observed in some natural crude oils. Dinur et al. (1980) report $\delta^{34}S$ values of organic-sulfur kerogen in Ghareb Limestone of the Dead Sea area from −10.7‰ in the south (Negev) to + 8.3‰ in the north (Nebi Musa).

5. CONCLUSIONS

The present study reports quantities and stable isotopes on organic and inorganic sulfur species at different levels of thermal maturation and petroleum formation as simulated in laboratory-pyrolysis experiments. The following main conclusions have been made on the basis of these hydrous pyrolysis results for Type-IIS kerogen in the Ghareb Limestone.

1. The most dominant sulfur transformation is the generation of $H_2S_{(gas)}$, which accounts for as much as 70 wt % of the original organic sulfur. The H_2S_{gas} formed during pyrolysis is isotopically lighter than the sulfur in the kerogen and oil.
2. The early sulfides released are up to 21‰ depleted in ^{34}S relative to the original unheated kerogen. These early-generated sulfides react with available metals and reach equilibrium with other sulfur species in the system. This results in narrowing of the isotopic differences between all active sulfur species.
3. Secondary pyrite that is isotopically heavier than the original pyrite forms from the early sulfides released by the decomposition of kerogen at experimental temperatures equal to or less than 300°C. As a result, the $\delta^{34}S$ of the total pyrite becomes ^{34}S enriched by as much as 8.3 ‰.
4. At experimental temperatures above 300°C, secondary pyrite begins to preferentially decompose relative to the original pyrite. As a result, the $\delta^{34}S$ of the total pyrite becomes ^{34}S depleted by as much as 6.2 ‰.
5. Caution should be used in reconstructing diagenetic conditions based on $\delta^{34}S$ of pyrite and kerogen in thermally mature source rocks. Formation and decomposition of isotopically heavy secondary pyrite during thermal maturation can mask the $\delta^{34}S$ of the original diagenetic pyrite.
6. With the increase of temperature, the organically bonded sulfur is enriched in ^{34}S by as much as 2‰ compared with the initial $\delta^{34}S$ values. Differences in $\delta^{34}S$ between kerogen, bitumen and expelled-oil are within 1‰.
7. The main transformations of kerogen-to-bitumen and bitumen-to-oil are reflected in the sulfur content and $\delta^{34}S$ of each phase, as well as in the amount and $\delta^{34}S$ of the generated $H_2S_{(gas)}$. These changes can be attributed in part to the breakage of different C-C, C-S, and S-S bond types.
8. $\delta^{34}S$ values can be used in oil-oil correlations, but the lack of a correlation may indicate mineral facies changes in the maturing source rock or a more open-system during thermal maturation. More open systems are expected to have greater differences in $\delta^{34}S$ values of oils at different thermal maturities.
9. If sufficient information is available on the major sulfur species (e.g., kerogen, oil, pyrite, H_2S and sulfate), then differences in their $\delta^{34}S$ values may be used to evaluate the openness of a thermally maturing system.
10. No TSR or formation of sulfate was observed under our experimental conditions.
11. The presence of water in the experiments at 340°C did not make a significant difference in the amount or $\delta^{34}S$ of the generated H_2S relative to the dry pyrolysis experiment. However, it did make a significant difference in the amount of the sulfur retained in the kerogen by more than a factor of two and a difference in $\delta^{34}S$ of 0.6‰.

Acknowledgments—The authors wish to thank Eli Tannenbaum of Kimron Oil & Minerals for promoting this collaborative project and for helpful suggestions. Michele Tuttle and Cyrus Berry of the USGS are appreciated for their invaluable analytical support in sulfur speciation as well as fruitful discussions. Appreciation is extended to Michael Prible, Pam Gemery-Hill and Augusta Warden of the USGS for technical assistance in elemental analyses, supplemental $\delta^{34}S$ determinations, and gas analyses, respectively. Alon Amrani thanks the European Association of Organic Geochemists (EAOG) for the Student Travel Award that enabled his work at the USGS in Denver. The Rieger Foundation is also gratefully acknowledged for Alon Amrani's Ph.D. Study Award. We also thank the Israel Academy of Sciences and the Minerva Foundation for the GC-EA-IRMS instrument, which was used for the $\delta^{34}S$ determinations in this study. Reviewers Geoffrey Ellis, David Manning, Richard Worden, Michele Tuttle and John Curtis are thanked for their suggestions and helpful comments.

Associate editor: J. Seewald

REFERENCES

Acholla F. and Orr W. L. (1993) Pyrite removal from kerogen without altering organic matter: The chromous chloride method. *Energy Fuels* **7,** 406–410.

Aizenshtat Z., Krein E. B., Vairavamurthy M. A. A. and Goldstein T. P. (1995) Role of sulfur in the transformations of sedimentary organic matter: A mechanistic overview. In *Geochemical Transformation of Sedimentary Sulfur* (eds. M. A. A. Vairavamurthy and A. Schoonen), pp. 16–39. Symposium Series 612. American Chemical Society.

Aizenshtat Z. and Amrani A. (2004a) Significance of $\delta^{34}S$ and evaluation of its imprint on sedimentary organic matter I. The role of reduced sulfur species in the diagenetic stage: A conceptual review. In *Geochemical Investigations: A Tribute to Isaac R. Kaplan* (eds. R. J. Hill et al.), pp. 15–33. Special Publication 8. Geochemical Society.

Aizenshtat Z. and Amrani A. (2004b) Significance of $\delta^{34}S$ and evaluation of its imprint on sedimentary organic matter II. Thermal changes of Type II-S kerogens catagenetic stage controlled mechanisms. Study and conceptual overview. In *Geochemical Investi-*

gations: A Tribute to Isaac R. Kaplan (eds. R. J. Hill et al.), pp. 35–50. Special Publication 8. Geochemical Society.

Amrani A. and Aizenshtat Z. (2004) Mechanisms of sulfur introduction chemically controlled: $\delta^{34}S$ imprint. *Org. Geochem.* **35,** 1319–1336.

Amrani A., Said Ahmad W., Lewan M. D., and Aizenshtat Z. (2005a) The $\delta^{34}S$ values of the early-cleaved sulfur upon thermal alterations as determined by closed and open systems pyrolyses. 22nd International Meeting of Organic Geochemists (IMOG) Seville, Spain, abstracts book part 1, pp. 290–291.

Amrani A., Said Ahmad W., and Aizenshtat Z. (2005b) The $\delta^{34}S$ values of the early-cleaved sulfur upon low temperature pyrolysis of a synthetic polysulfide cross-linked polymer. *Org. Geochem.* **36,** 971–974.

Anderson T. F. and Pratt L. M. (1995) Isotopic evidence for the origin of organic sulfur and elemental sulfur in mrine sediments. In *Geochemical Transformation of Sedimentary Sulfur* (eds. M. A. A. Vairavamurthy and A. Schoonen), pp. 378–396. Symposium Series 612. American Chemical Society.

Baskin D. K. and Peters K. E. (1992) Early generation characteristics of a sulfur-rich Monterey kerogen. *Am. Assoc. Petrol. Geol.* **76,** 1–13.

Bottcher M. E., Smock A., and Cypoinka H. (1998) Sulfur isotopes fractionation during experimental precipitation of iron (II) sulfide and manganese (II) sulfide at room temperature. *Chem. Geol.* **146,** 127–134.

Boulegue J. (1978) Solubility of elemental sulfur in water at 298 K. *Phophorous Sulfur Related Elements* **5,** 127–128.

Boulegue J. and Michard G. (1978) Constantes de formation des ions polysulfides S_6^{2-}, S_5^{2-} et S_4^{2-} en phase aqueuese. *Fr. Hydrol*. **9,** 27–33.

Coplen T. B. (1993) Uses of environmental isotopes. In *Regional Ground-Water Quality* (ed. W. M. Alley), pp. 227–254. Van Nostrand Reinhold.

Dinur D., Spiro B., and Aizenshtat Z. (1980) The distribution and isotopic composition of sulfur in organic rich sedimentary rocks. *Chem. Geol.* **31,** 37–51.

Fossing H. and Jorgensen B. B. (1990) Isotope exchange reactions with radio labeled sulfur compounds in anoxic seawater. *Biogeochemistry* **9,** 223–245.

Gaffney J. S., Premuzic E. T., and Manowitz B. (1980) On the use of sulfur isotope ratios in crude oil correlations. *Geochim. Cosmochim. Acta* **44,** 135–139.

Goldhaber M. B. (2004) Sulfur rich sediments. In *Treatise of Geochemistry,* 7 (ed. F. T. Mackenzie), pp. 257–288. Elsevier.

Idiz E. F., Tannenbaum E. and Kaplan I. R. (1990) Pyrolysis of high-sulfur Monterey kerogens—Stable isotopes of sulfur, carbon and hydrogen. In *Geochemistry of Sulfur in Fossil Fuels* (eds. W. L. Orr and C. M. White), pp. 575–591. Symposium Series 429. American Chemical Society.

Koopmans M. P., Rijipstra W. I. C., de Leeuw J. W., Lewan M. D., and Sinninghe Damsé J. S. (1998) Artificial maturation of immature sulfur-and organic matter-rich limestone fron the Ghareb Formation, Jordan. *Org. Geochem.* **28,** 503–521.

Krein E. B. (1993) Organic sulfur in the geosphere: Analysis, structures and chemical processes. In *The Chemistry of the Sulphur-Containing Functional Groups*. Suppl. S (eds. S. Patai and Z. Rappoport), pp. 975–1032. Wiley.

Krein E. B. and Aizenshtat Z. (1995) Proposed thermal pathways for sulfur transformation in organic simulation macromolecules: Laboratory simulation experiments. In *Geochemical Transformation of Sedimentary Sulfur* (eds. M. A. A. Vairavamurthy and A. Schoonen), pp. 110–137. Symposium Series 612. American Chemical Society.

Lewan M. D. (1983) Effects of thermal maturation on stable organic carbon isotopes as determined by hydrous pyrolysis of Woodford Shale. *Geochim. Cosmochim. Acta* **47,** 1471–1479.

Lewan M. D. (1985) Evaluation of petroleum generation by hydrous pyrolysis experimentation. *Phil. Trans. R. Soc. Lond.* **315,** 123–134.

Lewan M. D. (1986) Stable carbon isotopes of amorphous kerogens from Phanerozoic sedimentary rocks. *Geochim. Cosmochim. Acta* **50,** 1583–1591.

Lewan M. D. (1993) Laboratory simulation of petroleum formation: Hydrous pyrolysis. In *Organic Geochemistry* (eds. M. H. Engel and S. A. Macko), pp. 419–442. Plenum Press.

Lewan M. D. (1997) Experiments on the role of water in petroleum formation. *Geochim. Cosmochim. Acta* **61,** 3691–3723.

Lewan M. D. (1998) Sulfur-radical control on petroleum formation rates. *Nature* **391,** 164–166.

Manowitz B., Krouse H. R., Barker C. and Premuzic E. T. (1990) Sulfur isotope data analysis of crude oils from the Bolivar coastal fields (Venezuela). In *Geochemistry of Sulfur in Fossil Fuels* (eds. W. L. Orr and C. M. White), pp. 592–612. Symposium Series 429. American Chemical Society.

Minster T., Nathan Y., and Raveh A. (1992) Carbon and sulfur relationships in marine Senonian organic-rich, iron-poor sediments from Israel—A case study. *Chem. Geol.* **97,** 145–161.

Nelson B. C., Eglinton T. I., Seewald J. F., Vairavamurthy M. A. and Miknis F. P. (1995) Transformations in organic sulfur speciation during maturation of Monterey shale: Constraints from laboratory experiments. In *Geochemical Transformation of Sedimentary Sulfur* (eds. M. A. A. Vairavamurthy and A. Schoonen), pp. 138–166. Symposium Series 612. American Chemical Society.

Orr W. L. (1974) Changes in sulfur content and isotopic ratios of sulfur during petroleum maturation study of Big Horn Basin Plaeozoic oils. *Am. Assn. Petrol. Geol. Bull.* **50,** 2295–2318.

Orr W. L. (1986) Kerogen/asphaltene/sulfur relationships in sulfur-rich Monterey oils. *Org. Geochem.* **10,** 499–516.

Price F. T. and Shieh Y. N. (1979) Fractionation of sulfur isotopes during laboratory synthesis of pyrite at low temperatures. *Chem. Geol.* **27,** 245–253.

Schwarzenbach G. and Fisher A. (1960) Aciditat der sulfane und die zusammensetzung wasseriger polysulfidlosungen. *Helv. Chim. Acta* **43,** 1365–1390.

Seewald J. S. (2001) Aqueous geochemistry of low molecular weight hydrocarbons at elevated temperatures and pressures: Constrains from mineral buffered laboratory experiments. *Geochim. Cosmochim. Acta* **65,** 1641–1664.

Seewald J. S. (2003) Organic-inorganic interactions in petroleum-producing sedimentary basins. *Nature* **426,** 327–333.

Seewald J. S., Seyfried E. Jr., and Shanks W. C. III. (1994) Variations in the chemical and stable isotope composition of carbon and sulfur species during organic-rich sediment alteration: An experimental and theoretical study of hydrothermal activity at guaymas basin, gulf of California. *Geochim. Cosmochim. Acta* **58,** 5065–5082.

Shahar Y. and Wurzburger U. (1967) A new oil shale deposit in the northern Negev. In *Seventh World Petroleum Congress Proceedings,*Vol. 3, pp. 719–728. Elsevier.

Spiro B. (1980). Geochemistry and mineralogy of bituminous rocks in Israel. Ph.D. thesis. Hebrew University of Jerusalem.

Spiro B., Dinur D., and Aizenshtat Z. (1983a) Evaluation of source, environments of deposition and diagenesis of some Israeli "oil shales": N-alkanes, fatty acids, tetrapyrroles and kerogen. *Chem. Geol.* **39,** 189–214.

Spiro B., Welte D. H., Rullkotter J., and Schaeffer R. G. (1983b) Asphalts, oils and bituminous rocks from the Dead Sea Area: A geochemical correlation study. *Am. Assoc. Petrol. Geol.***67,** 1163–1175.

Staudt W. J. and Schoonen M. A. A. (1995) Sulfate incorporation into sedimentary carbonates. In *Geochemical Transformation of Sedimentary Sulfur* (eds. M. A. A. Vairavamurthy and A. Schoonen), pp. 332–345. Symposium Series 612. American Chemical Society.

Stoler A., Spiro B., Amrani A., and Aizenshtat Z. (2003) Evaluation of $\delta^{34}S$ changes during stepwise pyrolysis of bituminous rocks and Type II-S Kerogen. 21st International Meeting of Organic Geochemists (IMOG) Krakow, Poland, abstracts book part 1, pp. 103–104.

Suleimenov O. M. and Krupp R. E. (1994) Solubility of hydrogen sulfide in pure water and in NaCl solutions, from 20 to 320C and at saturation pressures. *Geochim. Cosmochim. Acta* **58,** 2433–2444.

Tannenbaum E. and Aizenshtat Z. (1984) Formation of immature asphalt from organic-rich carbonate rocks—2: Correlation of mat-

uration indicators. In *Advances in Organic Geochemistry 1983* (eds. P. A. Schenck, J. W. de Leeuw, and G. W. M. Lijmback). *Org. Geochem.* **6,** 503–511.

Tannenbaum E. and Aizenshtat Z. (1985) Formation of immature asphalt from organic-rich carbonate rocks—I. Geochemical correlation. *Org. Geochem.* **8,** 181–192.

Thode H. G. (1981) Sulfur isotope ratios in petroleum research and exploration: Williston Basin. *Am. Assn. Petrol. Geol. Bull.* **65,** 1527–1535.

Thode H. G., Monster J., and Dunford H. B. (1958) Sulphur isotope abundances in petroleum and associated materials. *Am. Assn. Petrol. Geol. Bull.* **42,** 2619–2641.

Thode H. G. and Monster J. (1970) Sulfur isotope abundances and genetic relations of oil accumulations in the Middle East. *Am. Assn. Petrol. Geol. Bull.* **54,** 627–637.

Tuttle M. L., Goldhaber M. B., and Williamson D. L. (1986) An analytical scheme for determining forms of sulfur in oil shales and associated rocks. *Talanta* **33,** 953–961.

Vredenburgh L. D. and Cheney E. S. (1971) Sulphur and carbon isotopic investigation of petroleum, Wind River Basin, Wyoming. *Am. Assn. Petrol. Geol. Bull.* **55,** 1954–1975.

Waples D. W. and Curiale J. A. (1999) Oil-oil and oil-source rock correlations. In *Exploring for Oil and Gas Traps* (eds. E. A. Beaumont and N. H. Foster), pp. 8-1 to 8-71. American Association of Petroleum Geology, Tulsa.

Wilkin R.T. and Barnes H.L. (1996) Pyrite formation by reactions of iron monosulfides with dissolved inorganic and organic species. *Geochim. Cosmochim. Acta* **60,** 4167–4179.

Worden R.H., Smalley P.C., and Barclay S.A. (2003) H_2S and diagenetic pyrite in North Sea sandstones: Due to TSR or organic sulphur compound cracking? *J. Geochem. Exp.* **4022,** 1–5.

Zaback D.A. and Pratt L.M. (1992) Isotopic composition and speciation of sulfur in Miocene Monterey Formation: Re-evaluation of sulfur reactions during early diagenesis in marine environments. *Geochim. Cosmochim. Acta* **56,** 763–774.